

Robust, durable gene activation *in vivo* via mRNA-encoded activators

Jared P. Beyersdorf^{1,‡}, Swapnil Bawage^{1,‡}, Nahid Iglesias^{2,‡}, Hannah E. Peck¹, Ryan A. Hobbs¹, Jay A. Wroe¹, Chiara Zurla¹, Charles A. Gersbach^{2,3,4}, and Philip J. Santangelo^{1,*}

Supplementary Tables and Figures

Supplementary Tables

Table S1: Sequences of sgRNA used in the study

B4galnt2 sgRNA	Sequence (5' - 3')
1	mC*mA*mC*rArUrCrCrUrGrGrArCrGrCrGrArGrGrCrA
2	mC*mU*mA*rUrUrUrArArGrUrUrGrGrUrCrCrArCrUrG
3	mU*mG*mG*rArArCrArCrArUrCrCrUrGrGrArCrGrCrG
4	mG*mC*mG*rUrCrCrArGrGrArUrGrUrGrUrUrCrCrArA
5	mG*mU*mU*rGrGrUrCrCrArCrUrGrUrGrGrCrUrGrUrG
Non Target	mG*mC*mA*rCrUrArCrCrArGrArGrCrUrArArCrUrCrA
Epo sgRNA	Sequence (5' - 3')
1	mC*mC*mC*rUrGrGrCrCrArArGrGrGrUrCrCrGrUrUrC
2	mU*mG*mA*rGrArCrArCrArGrCrCrArCrCrGrGrCrCrA
3	mU*mG*mU*rCrUrCrArCrUrGrUrGrUrUrCrCrCrGrArA
4	mC*mC*mC*rGrArArCrGrGrArCrCrCrUrUrGrGrCrCrA
5	mC*mC*mC*rUrGrGrCrCrArArGrGrGrUrCrCrGrUrUrC
Modified sgRNA scaffold	rGrUrUrUrUrArGrAmGmCmUmAmGmAmAmAmUrAmGmCrArArGrUrUrArArArArUrArArGrGrCrUrArGrUrCrCrGrUrUrArUrCrAmAmCmUmUmGmAmAmAmAmAmGmUmGmGmCmAmCmCmGmAmGmUmCmGmGmUmGmCmU*mU*mU

Abbreviations: r= ribonucleotide base, m=phosphorothioated 2' O-methyl ribonucleotide base, *= Phosphorothioate bond

Table S2: Gene activator protein coding sequences and mCherry DNA sequence

<p>VPH-dCas9-SS18 (Flag-tag, VP64, p65, HSF1, SV40 NLS, dCas9, SS18, T2A, mCherry)</p> <p>MDYKDHGDDYKDHIDYKDDDDKHVDALDDFDLDMGLGSDALDDFDLDMGLGSDALDDFDLDMGLGSDALDDFDLDMGLGSDALDDFDLDMGLGSLPSASVEFEGSGGPGSQISNQALALAPSSAPVLAQTMVPSSAMVPLAQPPAPAPVLTGPPQSL SAPVPKSTQAGEGTLSEALLHLQFDAEDL GALLGNSTDPGVFTDLASVDNSEFQQLLNQGVSMHSTAEPMLMEYPEAITRLVTGSQRPPDPAPTPLGTSGLPNGLSGDEDFSSIADMDFSALLSQISSSGQGGGGSGFSVDTSALLDLFSPSVTPDMSLPDL DSSLASIQELLSPQEPPRPPEAENSSPDSGKQLVHYTAQPLFLLDPGSVDTSNDLPVLFELGEGSYFSEGDFGAEDPTISLLTGSEPPKAKDPTVSNPKKKRKVGRGMDKKYSIGLAIGTNSV GWAVITDEYKVPSKFKVLGNTDRHSIKKNLIGALLFDSGETAEATRLKRTARRRYTRRKNRI CYLQEIFSNEMAKVDDSSFFHRLEESFLVEEDKKHERHPIFGNIVDEVAYHEKYPTIYHLRKKLV DSTDKADLRILIYALAHMIKFRGHFLIEGDLNPDNSDVKLFIQLVQTYNQLFEENPINASGVD AKAILSARLSKSRLENLIAQLPGEKKNLFGNLIALSLGLTPNFKSNFDLAEDAKLQLSKDTY DDDLNLALQIGDQYADLFLAAKNLSAILLSDILRVNTEITKAPLSASMIKRYDEHHQDLTLLK ALVRQQLPEKYKEIFFDQSKNGYAGYIDGGASQEEFYKFIKPILEKMDGTEELLVVLNRELL RKQRTFDNGSIPHQIHLGELHAILRRQEDFYFPLKDNREKIEKILTFRIPYYVGPLARGNSRFA WMTRKSEETITPWNFEVVDKGASAQSFIERMTNFDKNLPNEKVLPHKSLLEYFTVYNELT KVKYVTEGMRKPAFLSGEQKKAIVDLLFKTNRKVTVKQLKEDYFKKIECFDSVEISGVEDRFN ASLGTYHDLLKIKDKDFLDNEENEDILEDIVLTLTLFEDREMIEERLKYAHLFDDKVMKQLKR RRYTGWGRLSRKLINGIRDKQSGKTILDFLKSDGFANRNFMLIHDDSLTFKEDIQKAQVSG QGDSLHEHIANLAGSPAIKKILQTVKVVDELVKVMGRHKPENIVIAMARENQTTQKGQKNS RERMKRIEEGKELGSQILKEHPVENTQLQNEKLYLYLQNGRDMYVDQELDINRLSDYDVD AIVPQSFLKDDSIDNKVLRSDKNRGKSDNVPSEEVKKMKNYWRQLLNAKLITQRKFDNLT KAERGGELSEDKAGFIKRQLVETRQITKHVAQILDSRMNTKYDENDKLIREVKVITLKSCLVSD FRKDFQFYKVVREINNYHHAHDAYLNAVVG TALIKKYPKLESEFVYGDYKVYDVRKMIKSEQ EIGKATAKYFFYSNIMNFFKTEITLANGEIRKRPLIETNGETGEIVWDKGRDFATVRKVL SMPQ VNIVKKTEVQTGGFSKESILPKRNSDKLIARKKDWDPKKYGGFDSPTVAYSVLVAKVEK GK SKKLSVKELLGITIMERSSF EKNPIDFLEAKGYKEVKKDLIILPKYSLFELENGRKRMLASAG ELQKGNELALPSKYVNFLYLASHYEKLKGS PEDNEQKQLFVEQHKHYLDEIIEQISEFSKR VIL ADANLDKVL SAYNKH RDKPIREQAENIIHLFTLNLGAPAAFKYFDTTIDRKR YTSTKEVLDAT LIHQ SITGLYETRIDLSQLGGDSRADPKKKRKVASMSVAFAPRQRGKGEITPAAIQKMLDDN NHLIQCIMDSQNKGKTSECSQYQQLHTNLVYLATIADSNQNMQSLLPAPPTQNMMPMGPGG MNQSGPPPPRSHNMPSDGMVGGGPPAPHMQNQMNGQMPGNHMPMQGPGPNQLNM TNSSMNMPSSSHGSMGGYNHVPSSQSMPVQNQMTMSQGQPMGNYGPRPNMSMQPNQ GPMMHQQPPSQQYNMPQGGGQHYQQQPPMGMVGQVNQGNHMMGQRQIPPYRPPQQ GPPQQYSGQEDYYGDQYSHGGQGPPEGMNQYYPDGNSQYGGQQDAYQGPPPPQQGYP PQQQQYYPGQQGYPGQQQGYGPSQGGPGPQYPNYPQGQQQYGGYRPTQPGPPPPQ QRPYGYDQGQYGNYYQASGSGEGRGSLLTCGDVEENPGPMVSKGEEDNMAIIEKFMSFKV HMEGSVNGHEFEIEGEGEGRPYEGTQTAKLKVTGGPLPFAWDILSPQFMYGSKAYVKHPA DIPDYLKLSFPEGFKWERVMNFEDGGVVTVTQDSSLQDGEFIYKVKLRGTNFPDGPVMQK KTMGWEASSERMYPEDGALKGEIKQLKLDGGHYDAEVKTTYKAKKPVQLPGAYNVNIKL DITSHNEDYTIVEQYERAEGRHSTGGMDELYK*</p>
<p>dCas9-VP64 (dCas9, SV40 NLS, VP64, T2A, mCherry)</p>

MDKKYSIGLAIGTNSVGWAVITDEYKVPSSKFKVLGNTDRHSIKKNLIGALLFDSGETAEATRL
KRTARRRYTRRKNRICYLQEIFSNEMAKVDDSFHRLEESFLVEEDKKHERHPIFGNIVDEVA
YHEKYPTIYHLRKKLVDSTDKADLRLIYLALAHMIKFRGHFLIEGDLNPDNSDVKLFIQLVQTY
NQLFEENPINASGVDKAILSARLSKSRRENLIAQLPGEKKNGLFGNLIASLGLTPNFKSNF
DLAEDAQLQLSKDQYDDDLNLLAQIGDQYADLFLAAKNLSDAILLSDILRVNTEITKAPLSAS
MIKRYDEHHQDLTLLKALVRQQLPEKYKEIFFDQSKNGYAGYIDGGASQEEFYKFIKPILEKM
DGTEELLVKNREDLLRKQRTFDNGSIPHQIHLGELHAILRRQEDFYFPLKDNREKIEKILTFRI
PYYVGPLARGNSRFAWMTRKSEETITPWNFEVVDKGGASQAQSFIERMTNFDKNLPNEKVLP
KHSLLYEFYFTVYNELTKVKYVTEGMRKPAFLSGEQKKAIVDLLFKTNRKVTVKQLKEDYFKKI
ECFDSVEISGVEDRFNASLGTYHDLKIIKDKDFLDNEENEDILEDIVLTLTFEDREMIEERLK
TYAHLFDDKVMKQLKRRRYTGWGRLSRKLINGIRDKQSGKTILDFLKSDFANRNFQMQLIHD
DSLTFKEDIQKAQVSGQGDLSHEHIANLAGSPAIKKILQTVKVVDELVKVMGRHHPENIVIE
ARENQTTQKGQNSRERMKRIEKGELGSQILKEHPVENTQLQNEKLYLYLQNGRDMYV
DQELDINRLSDYDVAIVPQSFLKDDSIDNKVLRSDKNRGSNDNPSEEVVKMKMKNYWRQL
LNAKLITQRKFDNLTKAERGGLSELDKAGFIKRLVETRQITKHVAQILDSRMNTKYDENDKLI
REVKVITLKSCLVSDFRKDFQFYKREINNYHHAHDAYLNAVVGTAIKKYPKLESEFVYGDY
KVYDVRKMIKSEQEIGKATAKYFFYSNIMNFFKTEITLANGEIRKRPLIETNGETGEIVWDKG
RDFATVRKVLSPQVNIVKKTEVQTGGFSKESILPKRNSDKLIARKKDWDPKKYGGFDSPTV
AYSVLVAKVEKGSKSKLKSVEKLLGITIMERSSEFEKNPIDFLEAKGYKEVKKDLIILPKYSLF
ELENGRKRMLASAGELQKGNELALPSKYVNFLYLASHYEKLGSPEDNEQKQLFVEQHKHY
LDEIIIEQISEFSKRVLADANLDKVL SAYNKHRDKPIREQAENIIHLFTLTNLGAPAAFKYFDTTID
RKRYTSTKEVL DATLIHQ SITGLYETRIDLSQLGGDPIAGSKASPKKKRVGRADALDDFDLD
MLGSDALDDFDLMLGSDALDDFDLMLGSDALDDFDLMLASGSGEGRGSLTTCGDVEE
NPGPASGSGEGRGSLTTCGDVEENPGPMVSKGEEDNMAIIEFMSFKVHMEGSVNGHEFEI
EGEGEGRPYEGTQAKLVTKGGPLPFAWDILSPQFMYGSKAYVKHPADIPDYLKLSFPEGF
KWERVMNFEDGGVVTVDSSLDQGEFIYKVKLRGTNFPDGPVMQKKTMGWEASSERM
YPEDGALKGEIKQLKLDGGHYDAEVKTTYKAKKPVQLPGAYNVNIKLDITSHNEDYTIVEQ
YERAEGRHSTGGMDELYK*

dCas9-VPR (dCas9, SV40 NLS, VPR (VP64, RelA(p65), Rta), P2A, mCherry)

MDKKYSIGLAIGTNSVGWAVITDEYKVPSSKFKVLGNTDRHSIKKNLIGALLFDSGETAEATRL
KRTARRRYTRRKNRICYLQEIFSNEMAKVDDSFHRLSEESFLVEEDKKHERHPIFGNIVDEVA
YHEKYPTIYHLRKKLVDSTDKADLRLIYLALAHMIKFRGHFLIEGDLNPDNSDVKLFIQLVQTY
NQLFEENPINASGVDKAILSARLSKSRRENLIAQLPGEKKNGLFGNLIASLGLTPNFKSNF
DLAEDAQLQLSKDQYDDDLNLLAQIGDQYADLFLAAKNLSDAILLSDILRVNTEITKAPLSAS
MIKRYDEHHQDLTLLKALVRQQLPEKYKEIFFDQSKNGYAGYIDGGASQEEFYKFIKPILEKM
DGTEELLVKNREDLLRKQRTFDNGSIPHQIHLGELHAILRRQEDFYFPLKDNREKIEKILTFRI
PYYVGPLARGNSRFAMTRKSEETITPWNFEEVVDKGSASAQSFIERMTNFDKNLPNEKVLP
KHSLLYEYFTVYNELTKVKYVTEGMRKPAFLSGEQKKAIVDLLFKTNRKVTVKQLKEDYFKKI
ECFDSVEISGVEDRFNASLGTYHDLKIIKDKDFLDNEENEDILEDIVLTLTFEDREMIEERLK
TYAHLFDDKVMKQLKRRRYTGWGRLSRKLINGIRDKQSGKTILDFLKSDFANRNFQMQLIHD
DSLTFKEDIQKAQVSGQGDLSHEHIANLAGSPAIKKILQTVKVVDELVKVMGRHHPENIVEM
ARENQTTQKGQNSRERMKRIEKGELGSQILKEHPVENTQLQNEKLYLYLQNGRDMYV
DQELDINRLSDYDVAIVPQSFLKDDSIDNKVLRSDKARGKSDNVPSEEVVKKMKNYWRQL
LNAKLITQRKFDNLTKAERGGLSELDKAGFIKRLVETRQITKHVAQILDSRMNTKYDENDKLI
REVKVITLKSCLVSDFRKDFQFYKREINNYHHAHDAYLNAVVGTAIKKYPKLESEFVYGDY
KVYDVRKMIKSEQEIGKATAKYFFYSNIMNFFKTEITLANGEIRKRPLIETNGETGEIVWDKG
RDFATVRKVLSPQVNIKKTEVQTGGFSKESILPKRNSDKLIARKKDWDPKKYGGFDSPTV
AYSVLVAKVEKGSKKLKSVEKLLGITIMERSSSFENPIDFLEAKGYKEVKKDLIILPKYSLF
ELENGRKRMLASAGELQKGNELALPSKYVNFLYLASHYEKLGSPEDNEQKQLFVEQHKHY
LDEIIEQISEFSKRVLADANLDKVL SAYNKHRDKPIREQAENIIHLFTLTNLGAPAAFKYFDTTID
RKRYTSTKEVLDTLIHQSI TGLYETRIDLSQLGGDSRADPKKKRKV **SPGIRRLDALISTSLYK**
KAGYKEASGSGRADALDDFDLMLGSDALDDFDLMLGSDALDDFDLMLGSDALDDFDL
DMLINSRSSGSPKKKRKVGSYLPDTPDRHRIEERKRYETFKSIMKKS PFSGPTDPRPPP
RRIAVPSRSSASVPKPAPQYPFTSSLSTINYDEFPTMVFPSGQISQASALAPAPPQVLPQAP
APAPAPAMVSALAQAQAPVPVLPAGPPQAVAPPAPKPTQAGEGTLSEALLQLQFDDDLGA
LLGNSTDPVFTDLASVDNSEFQQLLNQGIPVAPHTTEPMLMEYPEAITRLVTGAQRPPDPA
PAPLGAPGLPNGLLSGDEDFSSIADMDFSALLGSGSGSRDSREGMFLPKPEAGSAISDVFEQ
REVCQPKRIRPFHPPGSPWANRPLPASLAPTPTGPVHEPVGSLTPAPVPQPLDPAPAVTPE
ASHLLEDPEETSQAVKALREMA DTVIPQKEEAICGQMDLSHPPPRGHLDLDTTLESMTD
DLNLDSP LPELNEILD TFLNDECLLHAMHISTGLSIFDTSLFGSGATNFSLLKQAGDVEENPG
PGSGATNFSLLKQAGDVEENPGPMVSKGEEDNMAIIEFMSFKVHMEGSVNGHEFEIEGEG
EGRPYEGTQAKLKVTKGGPLPFAWDILSPQFMYGSKAYVKHPADIPDYLLKLSFPEGFKWE
RVMNFEDGGVVTVTQDSSLQDGEFIYKVKLRGTNFPDGPVMQKKTMGWEASSERMYPED
GALKGEIKQRLKLDGGHYDAEVKTTYKAKKPVQLPGAYNVNIKLDITSHNEDYIVEQYERA
EGRHSTGGMDELYK*

dCas9-p300 (dCas9, **Nucleoplasmin NLS**, **p300**, **T2A**, **mCherry**)

MDKKYSIGLAIGTNSVGWAVITDEYKVPSKFKVLGNTDRHSIKKNLIGALLFDSGETAEATRL
KRTARRRYTRRKNRICYLQEIFSNEMAKVDDSFHRLSEESFLVEEDKKHERHPIFGNIVDEVA
YHEKYPTIYHLRKKLVDSTDKADLRLIYLALAHMIKFRGHFLIEGDLNPDNSDVKLFIQLVQTY
NQLFEENPINASGVDKAILSARLSKSRRENLIAQLPGEKKNGLFGNLIASLGLTPNFKSNF
DLAEDAQLQLSKDQYDDDLNLLAQIGDQYADLFLAAKNLSDAILLSDILRVNTEITKAPLSAS
MIKRYDEHHQDLTLLKALVRQQLPEKYKEIFFDQSKNGYAGYIDGGASQEEFYKFIKPILEKM
DGTEELLVKNREDLLRKQRTFDNGSIPHQIHLGELHAILRRQEDFYFPLKDNREKIEKILTFRI
PYYVGPLARGNSRFAWMTRKSEETITPWNFEVVDKGGASQAQSFIERMTNFDKNLPNEKVLP
KHSLLYEFYTVYNELTKVKYVTEGMRKPAFLSGEQKKAIVDLLFKTNRKVTVKQLKEDYFKKI
ECFDSVEISGVEDRFNASLGTYHDLKIIKDKDFLDNEENEDILEDIVLTLTFEDREMIEERLK
TYAHLFDDKVMKQLKRRRYTGWGRLSRKLINGIRDKQSGKTILDFLKSDFANRNFQMQLIHD
DSLTFKEDIQKAQVSGQGDSLHEHIANLAGSPAIKKILQTVKVVDELVKVMGRHHPENIVIE
ARENQTTQKGQKNSRERMKRIEKGELGSQILKEHPVENTQLQNEKLYLYLQNGRDMYV
DQELDINRLSDYDVAIVPQSFLKDDSIDNKVLRSDKNRKGSDNVPSEEVVKKMKNYWRQL
LNAKLITQRKFDNLTKAERGGLSELDKAGFIKRLVETRQITKHVAQILDSRMNTKYDENDKLI
REVKVITLKSCLVSDFRKDFQFYKREINNYHHAHDAYLNAVVGTAIKKYPKLESEFVYGDY
KVYDVRKMIKSEQEIGKATAKYFFYSNIMNFFKTEITLANGEIRKRPLIETNGETGEIVWDKG
RDFATVRKVLVSMQVNVKKEVQTTGGFSKESILPKRNSDKLIARKKDWDPKYYGGFDSPTV
AYSVLVVAKEKGSKLLKSVKELLGITIMERSSSFENPIDFLEAKGYKEVKKDLIILPKYSLF
ELENGRKRMLASAGELQKGNELALPSKYVNFYLASHYEKLGSPEDNEQKQLFVEQHKHY
LDEIIEQISEFSKRVLADANLDKVL SAYNKHRDKPIREQAENIIHLFTLTNLGAPAAFKYDFTTID
RKRYTSTKEVLDTLIHQITGLYETRIDLSQLGGDKRPAATKKAGQAKKKKGSIFKPEELRQ
ALMPTLEALYRQDPESLPFRQPVPDQLLGIPIYFDIVKSPMDLSTIKRKLDTGQYQEPWQYV
DDIWLMMFNNAWLYNRKTSRVYKYCSKLSEVFEQEIDPVMQSLGYCCGRKLEFSPQTLCCYG
KQLCTIPRDATYYSYQNRHYFCEKCFNEIQGESVSLGDDPSQPQTINKEQFSKRKNDTLDP
ELFVECTECGRKMHQICVLHHEIWPAGFVCDGCLKKSARTRKENKFSARLPSTRLGTFL
NRVNDFLRRQNHPESEGEVTVRVVHASDKTVEVKPGMKARFVDSGEMAESFPYRTKALFAF
EEIDGVDLCFFGMHVQEYGSDCPPPNQRRVYISYLDVHFFRPKCLRTAVYHEILIGYLEYVK
KLGYYTGHVACPPSEGGDYIFHCHPPDQKIPKPKRLQEWYKMLDKAVSERIVHDYKDIFK
QATEDRLTSAKELPYFEGDFWPNVLEESIKELEQEEEEERKREENTSNESTDVTKGDSKNAK
KNNKKTSKNKSSLRGNKKKPGMPNVSNDLSQKLYATMEKHKEVFFVIRLIAGPAANSPLPIV
DPDPLIPCDLMDGRDAFLTLARDKHLEFSSLRRAQWSTMCMMLVELHTQSQDGSSEGRGSLT
CGDVEENPGPGSEGRGSLTTCGDVEENPGPMVSKGEEDNMAIIEFMSFKVHMEGVSNGH
EFEIEGEGEGRPYEGTQTAKLKVTKGGPLPFAWDILSPQFMYGSKAYVKHPADIPDYKLSF
PEGFKWERVMNFEDGGVVTQDSSLQDGEFIYKVKLRGTNFPDGPVMMQKKTMGWEAS
SERMYPEDGALKGEIKQRLKLDGGHYDAEVKTTYKAKKPVQLPGAYNVNIKLDITSHNEDY
TIVEQYERAEGRHSTGGMDELYK*

AcrIIA4 (AcrIIA4, P2A, BFP)

MNLKELVREIKNKDYTAKLSGTDSNSITQLIIVNNDGNEYGISESNFESIVEKRVSTFENGWD
GAYEDEEEFYNDMQRDIVNRHFKGSGATNFSLLKQAGDVEENPGPGSGATNFSLLKQAGDV
EENPGPSELIKENMHMKLYMEGTVDNHHFKCTSEGEGKPYEGTQTMRIKVVGGPLPFAFD
ILATSFLYGSKTFINHTQGIPDFFKQSFPEGFTWERVTTYEDGGVLTATQDTSLQDGLIYNV
KIRGVNFTSNGPVMQKKTGLWEAFTETLYPADGGLEGRNDMALKLVGGSHLIANIKTTYRSK
KPAKNLKMPGVYVVDYRLERIKEANNETYVEQHEVAVARYCDLPSKLGHLN*

mCherry (DNA sequence)

ATGGTGAGCAAGGGCGAGGAGGATAACATGGCCATCATCAAGGAGTTCATGAGCTTCAA
GGTGACATGGAGGGCTCCGTGAACGGCCACGAGTTCGAGATCGAGGGCGAGGGCGA
GGCCCGCCCTACGAGGGCACCCAGACCGCCAAGCTGAAGGTGACCAAGGGTGGCCC
CCTGCCCTTCGCCTGGGACATCCTGTCCCCTCAGTTCATGTACGGCTCCAAGGCCTACG
TGAAGCACCCCGCCGACATCCCCGACTACTTGAAGCTGTCCTTCCCCGAGGGCTTCAAG
TGGGAGCGCGTGATGAACTTCGAGGACGGCGGCGTGGTGACCGTGACCCAGGACTCCT
CCCTGCAGGACGGCGAGTTCATCTACAAGGTGAAGCTGCGCGGCACCAACTTCCCCTC
CGACGGCCCCGTAATGCAGAAGAAAACCATGGGCTGGGAGGCCTCCTCCGAGCGGATG
TACCCCGAGGACGGCGCCCTGAAGGGCGAGATCAAGCAGAGGCTGAAGCTGAAGGAC
GGCGGCCACTACGACGCTGAGGTCAAGACCACCTACAAGGCCAAGAAGCCCGTGCAGC
TGCCCGGCGCCTACAACGTCAACATCAAGTTGGACATCACCTCCCACAACGAGGACTAC
ACCATCGTGGAACAGTACGAACGCGCCGAGGGCCGCCACTCCACCGGCGGCATGGAC
GAGCTGTACAAGTAGTAA

Table S3: Ordinary Two-way ANOVA & Post Test Results

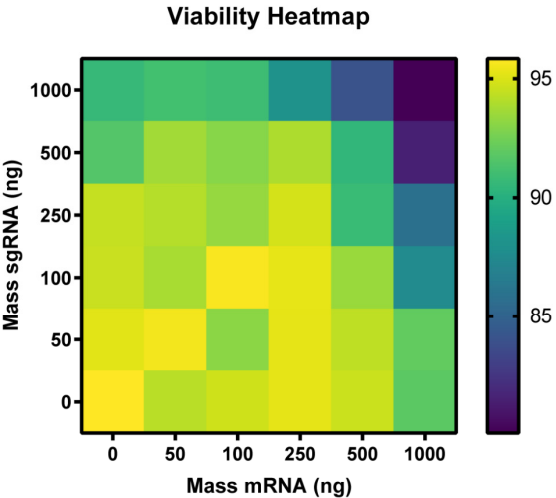
%mCherry+						
Ordinary Two-way ANOVA			Tukey's multiple comparisons test			
Source of Variation	% of total variation	P value	Comparison	Mean Diff.	95.00% CI of diff.	Adjusted P Value
Interaction	23.3	0.0051	VPR vs. VP64	-6.906	-12.34 to -1.467	0.0101
gRNA	12.32	0.0136	VPR vs. P300	-15.97	-21.41 to -10.53	<0.0001
Activator	37.99	<0.0001	VP64 vs. P300	-9.067	-14.51 to -3.628	0.0007
mCherry MFI						
Ordinary Two-way ANOVA			Tukey's multiple comparisons test			
Source of Variation	% of total variation	P value	Comparison	Mean Diff.	95.00% CI of diff.	Adjusted P Value
Interaction	15.17	<0.0001	VPR vs. VP64	-359.1	-449.9 to -268.2	<0.0001
gRNA	2.948	0.0596	VPR vs. P300	-632.8	-723.7 to -542.0	<0.0001
Activator	72.89	<0.0001	VP64 vs. P300	-273.8	-364.6 to -182.9	<0.0001

Table S5: Primer-Probe set used in the study

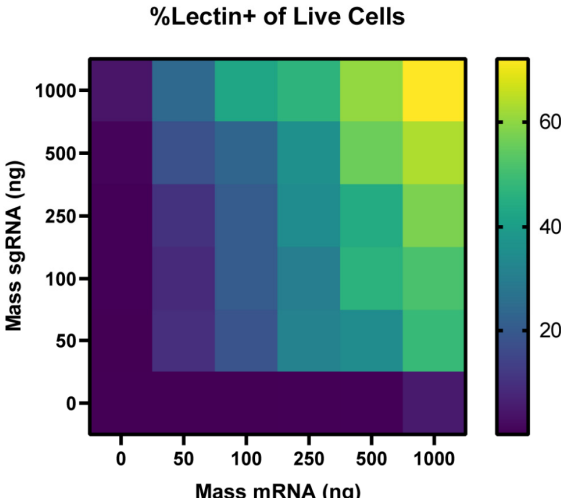
Gene	Primer Probe set ID	Forward primer	Reverse primer	TaqMan probe
B4galnt2	Mm00484661_m1	-	-	-
Epo	Mm01202755_m1			
Gapdh	Mm99999915_g1	-	-	-
mCherry	-	TGAGGTCAAGA CCACCTACA	CTGTTCCAC GATGGTGT AGTC	TTGGACATCACCTCC CACAACGAG

Supplementary Figures

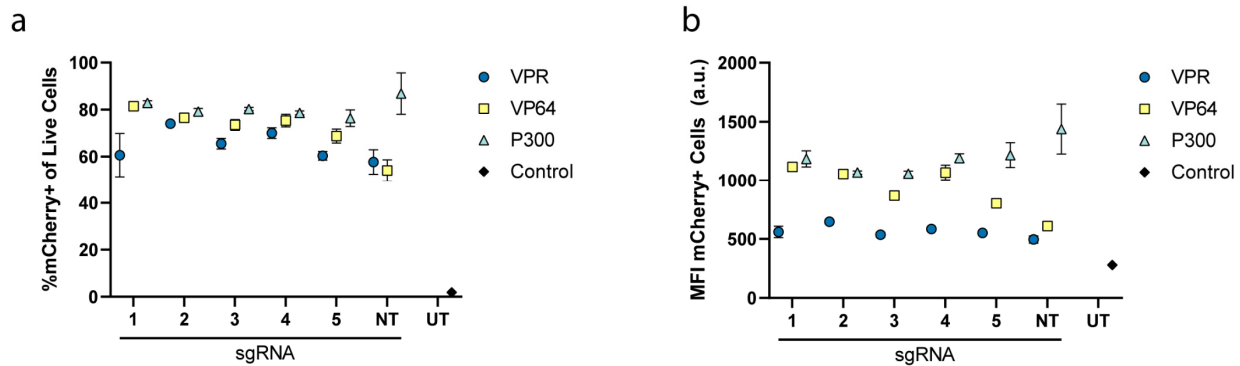
a



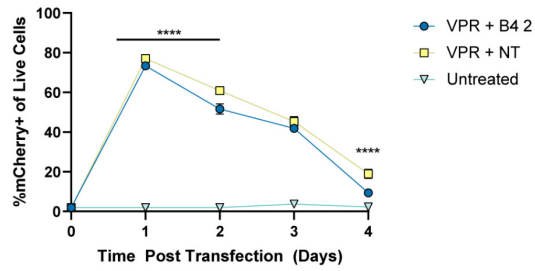
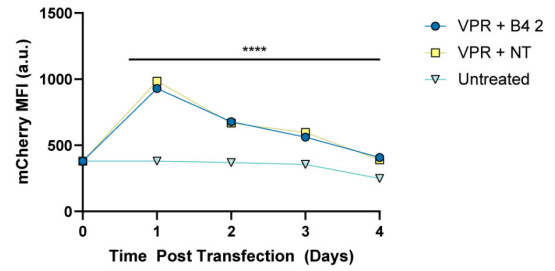
b



Sup. Fig. 1 | *In vitro* dose optimization in AML12 cells by flow cytometry. a, Heatmap showing the percentage of live cells (a) and lectin+ cells (b) with varying doses of VPR mRNA and sgRNA

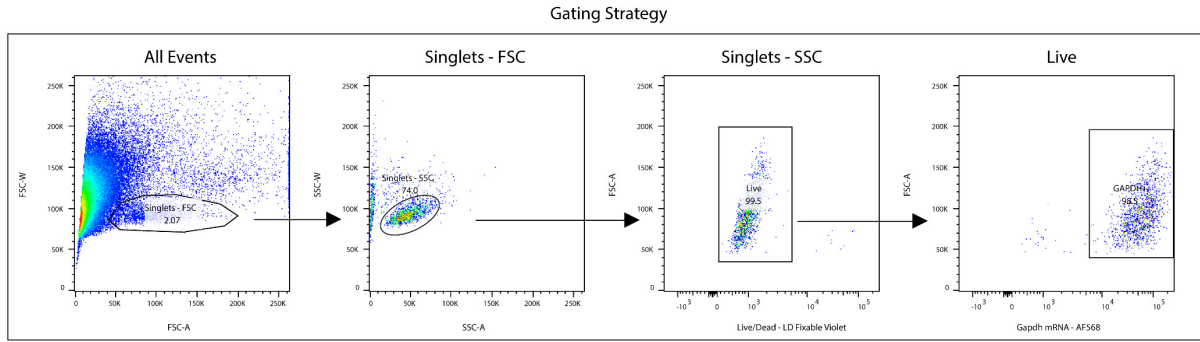


Sup. Fig. 2 | mCherry expression from in vitro activator screen. Each activator mRNA construct contained a cleavable mCherry sequence. **a**, Percentage of mCherry+ cells. **b**, MFI of mCherry+ cells. To assess differences in protein expression between the activator mRNA constructs, an ordinary two-way ANOVA was performed with Tukey's multiple comparisons test (**Table S2**) Data represent mean \pm SEM ($n = 3$ biological replicates).

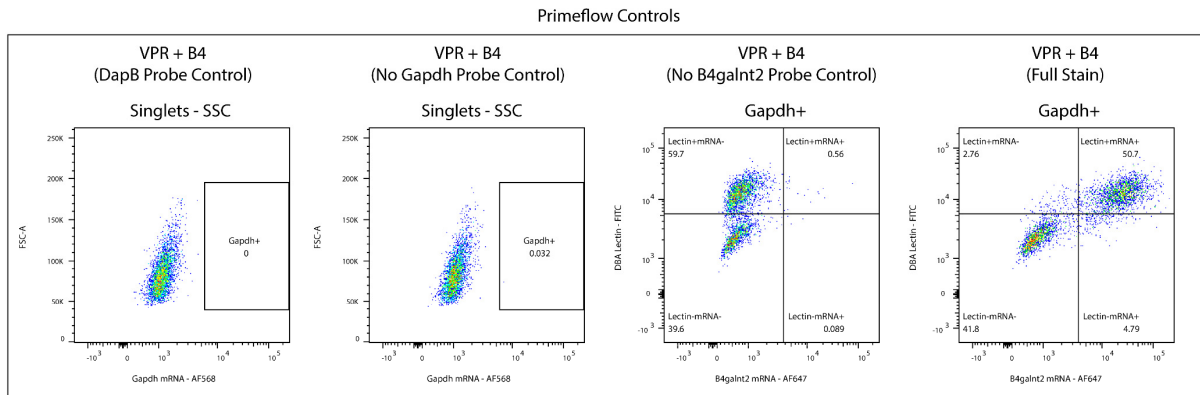
a**b**

Sup. Fig. 3 | mCherry expression from in vitro time course. Each activator mRNA construct contained a cleavable mCherry sequence. **a**, Percentage of mCherry+ cells over time. **b**, MFI of mCherry+ cells. To assess differences in protein expression between the activator mRNA constructs over time. An ordinary two-way ANOVA was performed with Tukey's multiple comparisons test. Data represent mean \pm SEM ($n = 3$ biological replicates).

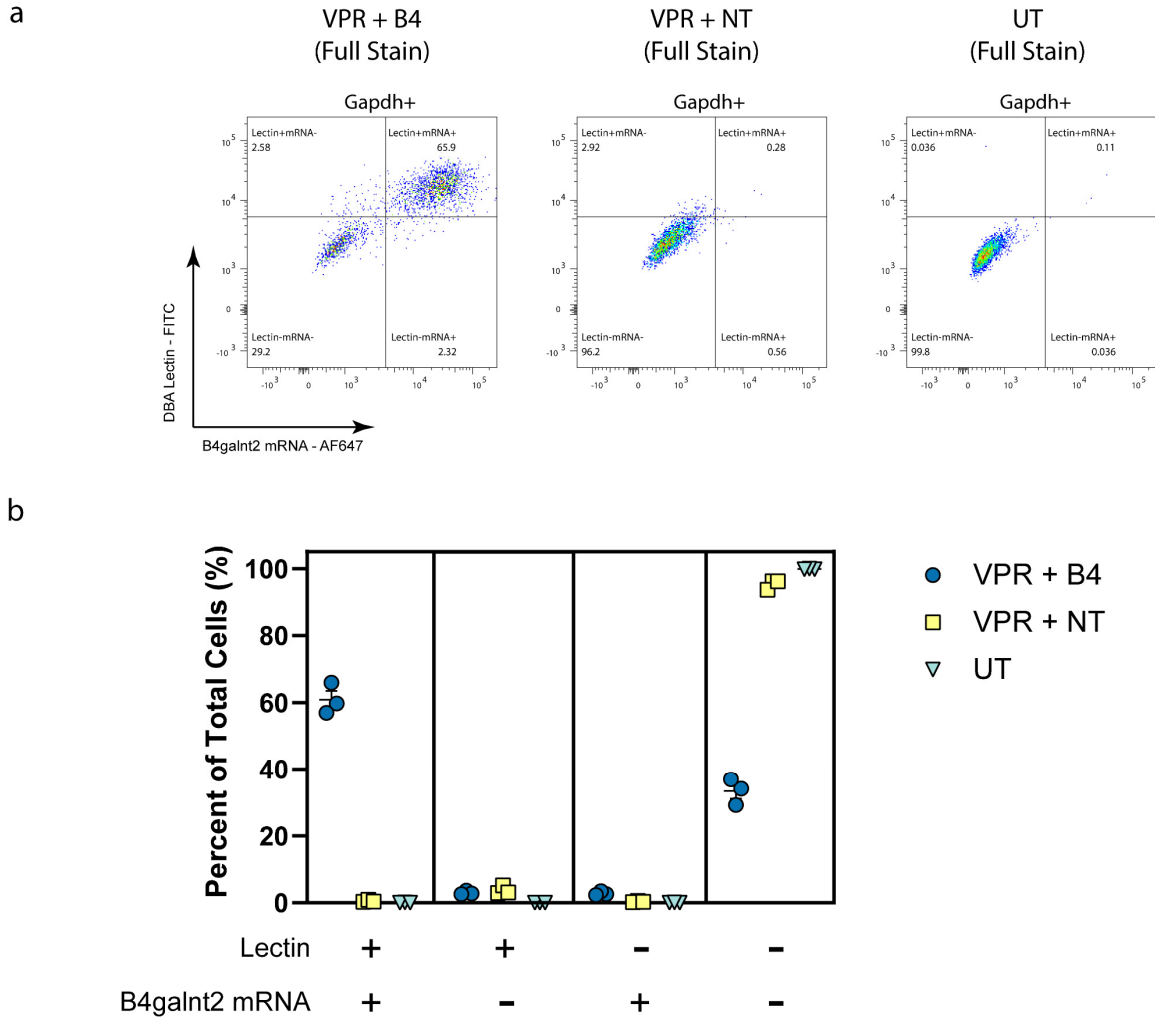
a



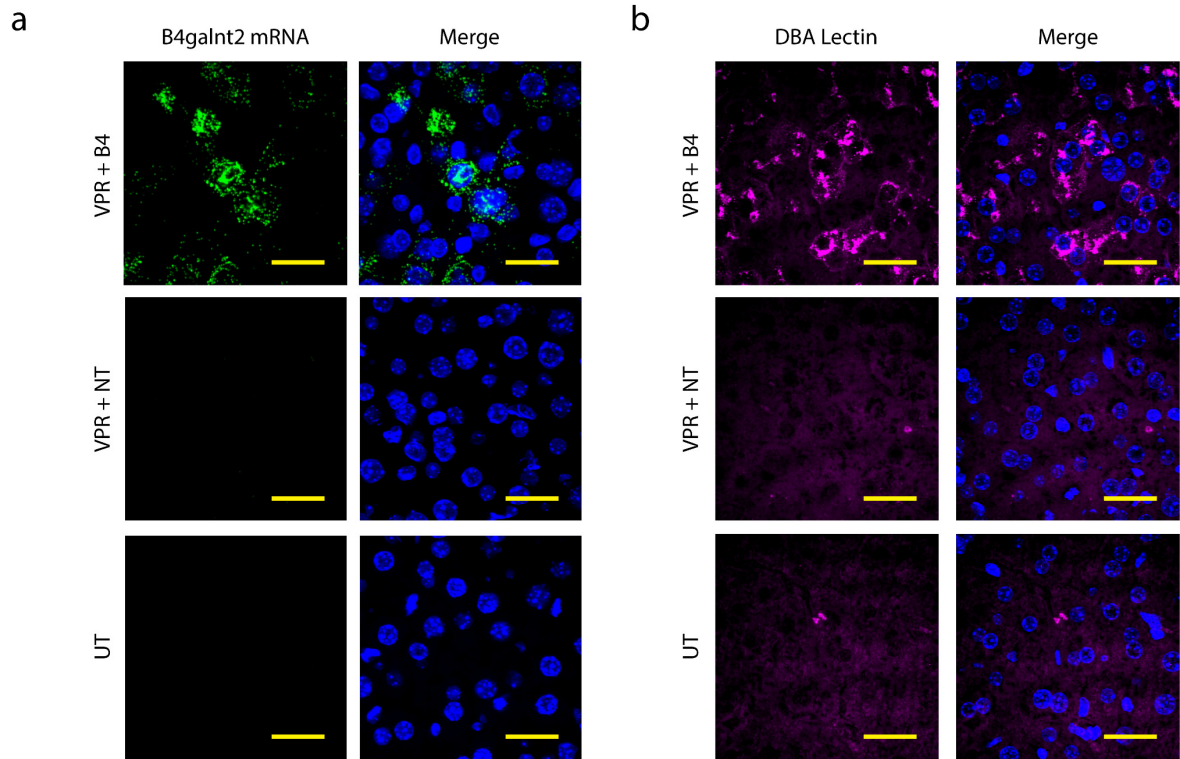
b



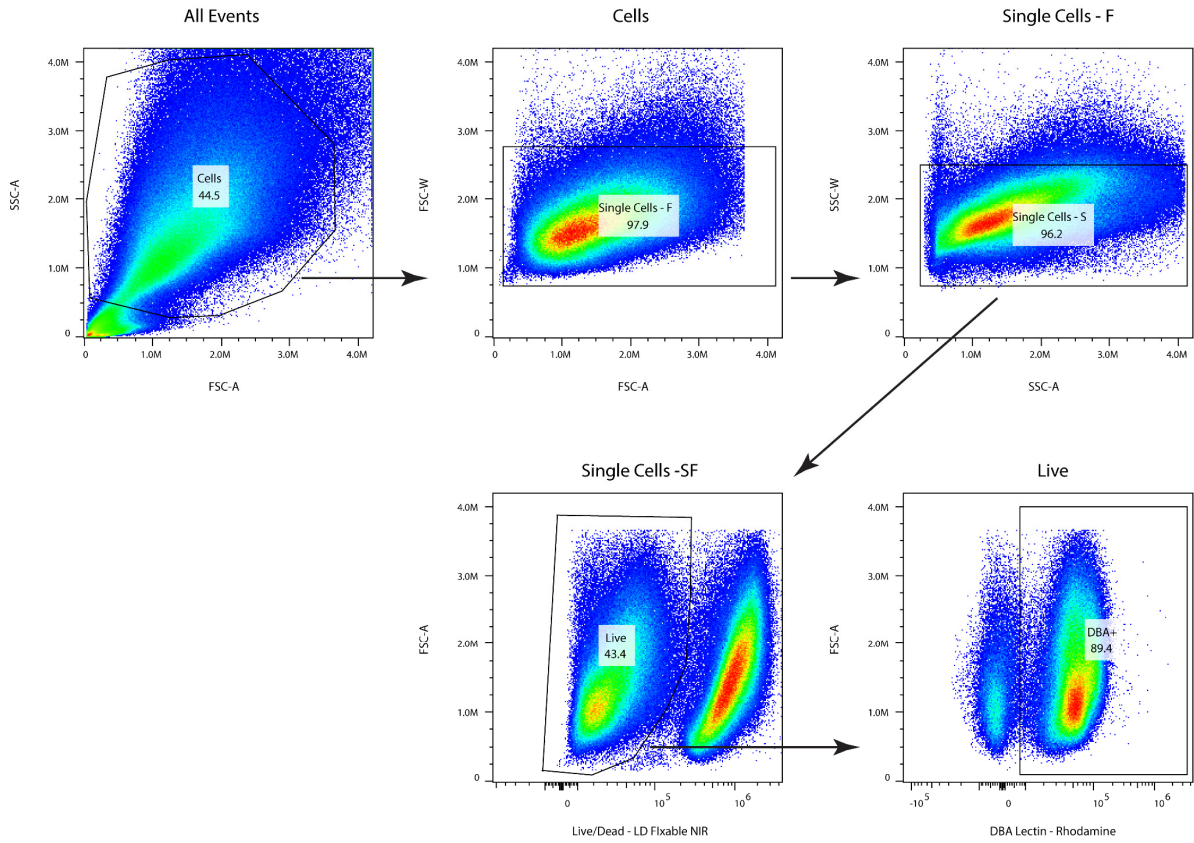
Sup. Fig. 4 | Flow cytometry gating scheme and controls for PrimeFlow assay in AML12 cells. a, Gating strategy b, PrimeFlow controls demonstrating probe specificity (DapB control and no Gapdh control) and successful DBA lectin staining with simultaneous PrimeFlow mRNA signal.



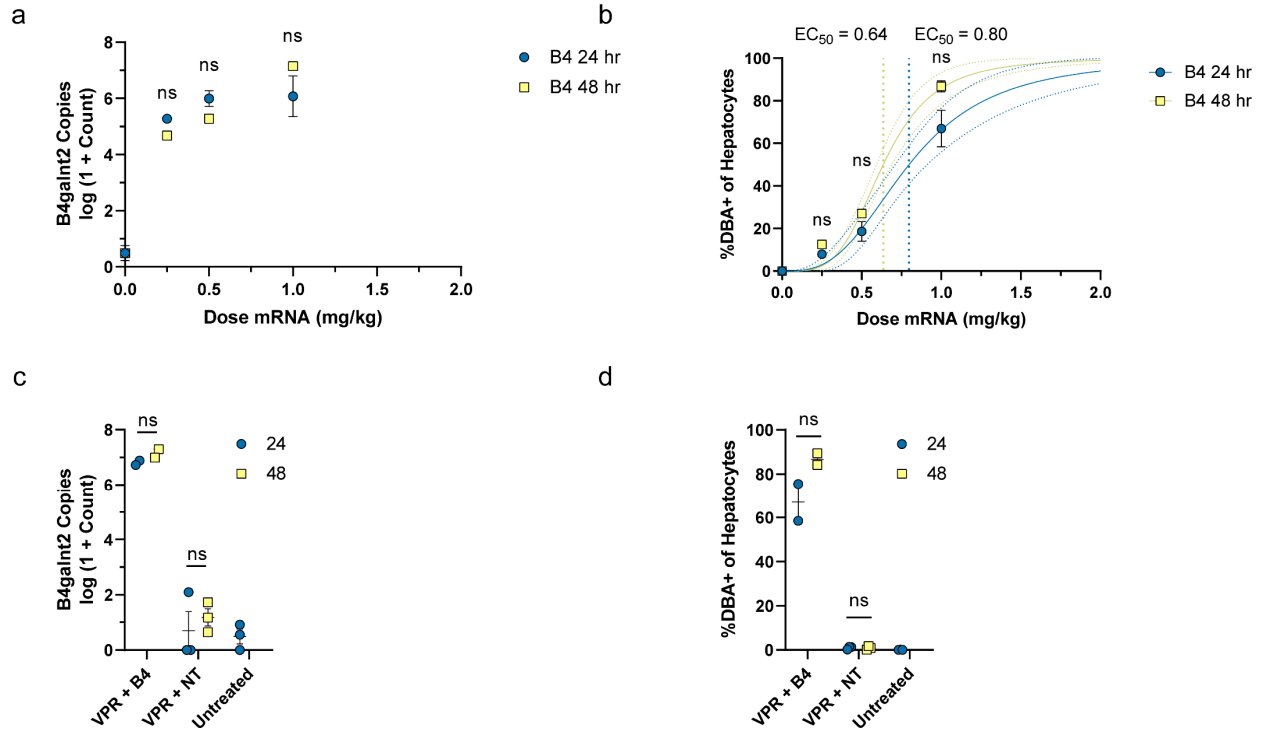
Sup. Fig. 5 | Demonstration of B4galnt2 mRNA upregulation by PrimeFlow in AML12 cells.
a, Representative flow plots depicting the cell populations observed between treatment conditions as defined by B4galnt2 mRNA signal and lectin staining. **b**, Quantification of the percentage of cells according to B4galnt2 mRNA upregulation and lectin staining status. Data represent mean \pm SEM (n = 3 biological replicates).



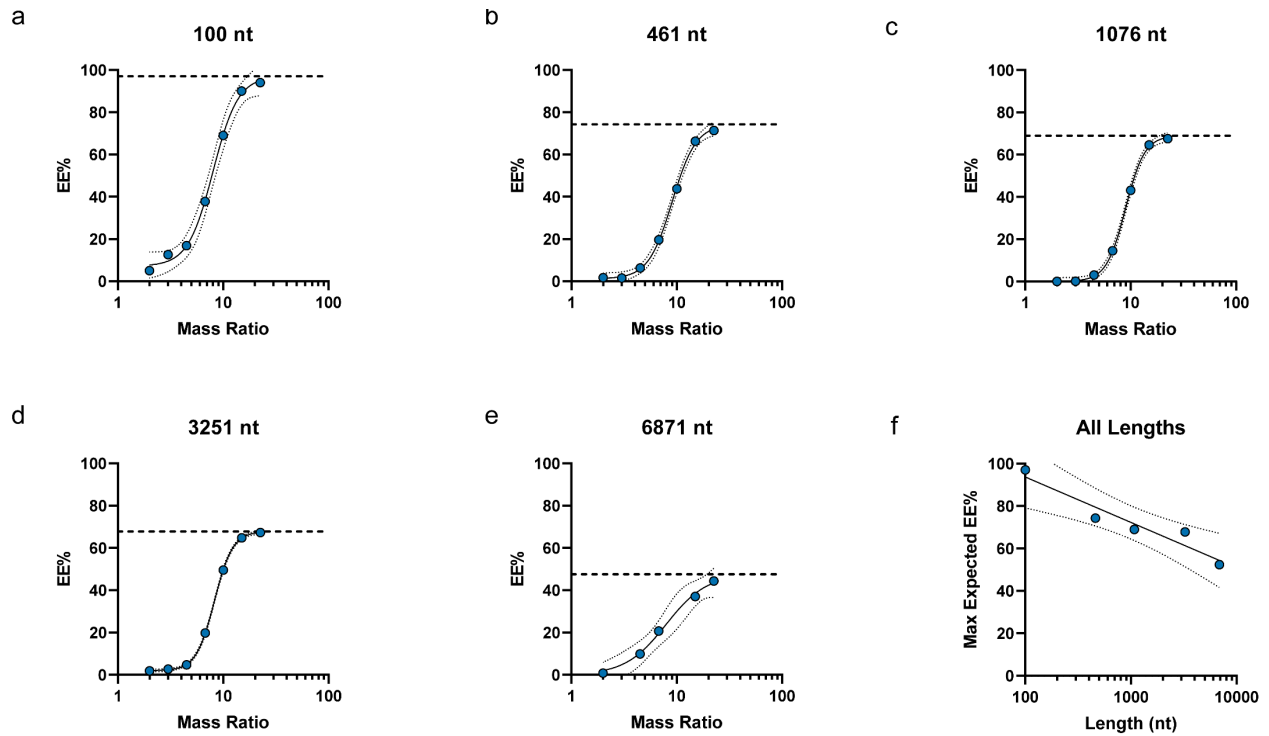
Sup. Fig. 6 | Initial demonstration of successful B4galnt2 gene activation in liver samples. Representative images showing RNAscope staining for B4galnt2 mRNA (green) (**a**), DBA lectin (magenta) (**b**), and DAPI (blue) at 1 day post injection. Scale bars are all 25 μ m



Sup. Fig. 7 | Flow cytometry gating scheme for hepatocytes from liver cell suspensions. Representative flow plots depict the gating strategy based on side-scatter and live/dead staining to gate on live hepatocytes.

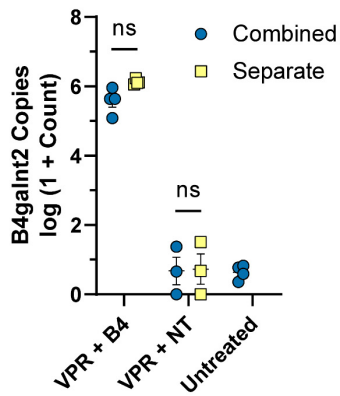


Sup. Fig. 8 | Initial dose response results using combined LNP formulation approach. B4galnt2 mRNA copy numbers (a) and percentage of activated hepatocytes (b) from liver cell suspensions at varying doses of VPR mRNA and B4-targeted sgRNA. (c,d) Comparison of B4galnt2 mRNA copy numbers and percentage of activated hepatocytes between treatment groups receiving either VPR mRNA + B4 sgRNA (1 mg/kg mRNA), VPR mRNA + NT sgRNA (1 mg/kg mRNA), or no treatment. Statistical significance was assessed using a two-way ANOVA followed by Dunnett's multiple comparison between 24 and 48 hours. (ns, $P > 0.05$). 4PL curves were fit to data in b (solid lines = best fit curve, dotted lines = 95% CI). An extra sum-of-squares F-test was performed to assess statistical significance between the EC₅₀ values. When $P > 0.05$, a combined EC₅₀ values was reported for the curves.

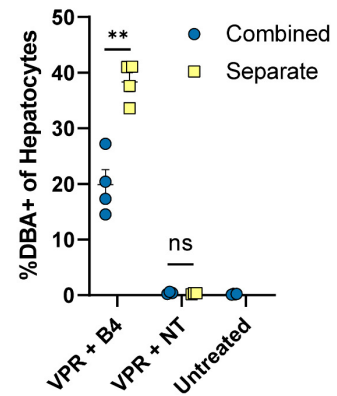


Sup. Fig. 9 | Mass ratio and mRNA length influence encapsulation efficiency of LNPs. Encapsulation efficiencies for cKK-E12 LNPs formulated with sgRNA (a) or different mRNAs with increasing lengths (b-e) at lipid:mRNA mass ratios ranging from 2 to 20. 4PL curves were fit to data in a-e (solid lines = best fit curve, dotted lines = 95% CI, horizontal dashed line = asymptotic top value). The asymptotic top values from each graph was plotted against RNA length (f), demonstrating a decrease in the theoretical maximum encapsulation efficiency with increasing length. Linear regression was performed for the combined data set ($R^2 = 0.913$, solid line = best fit, dotted lines = 95% CI). Pearson correlation analysis was also performed for the combined data set ($r = -0.955$, $P = 0.011$). All data points represent single replicates.

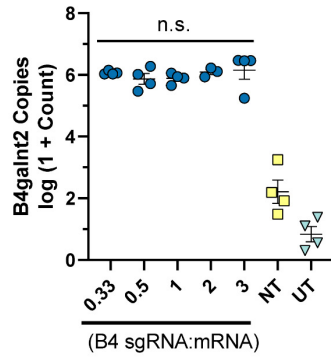
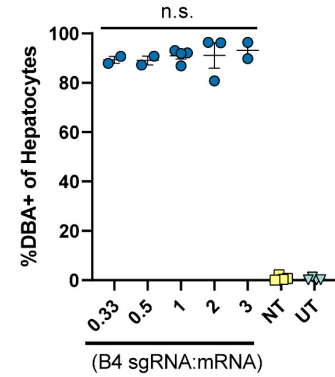
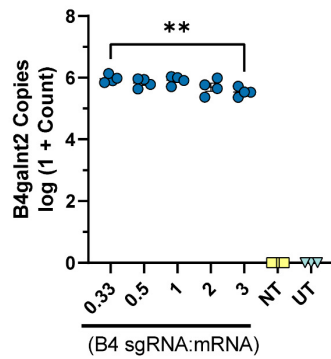
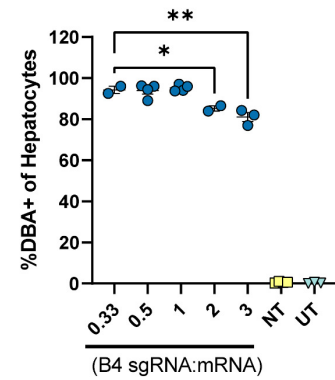
a



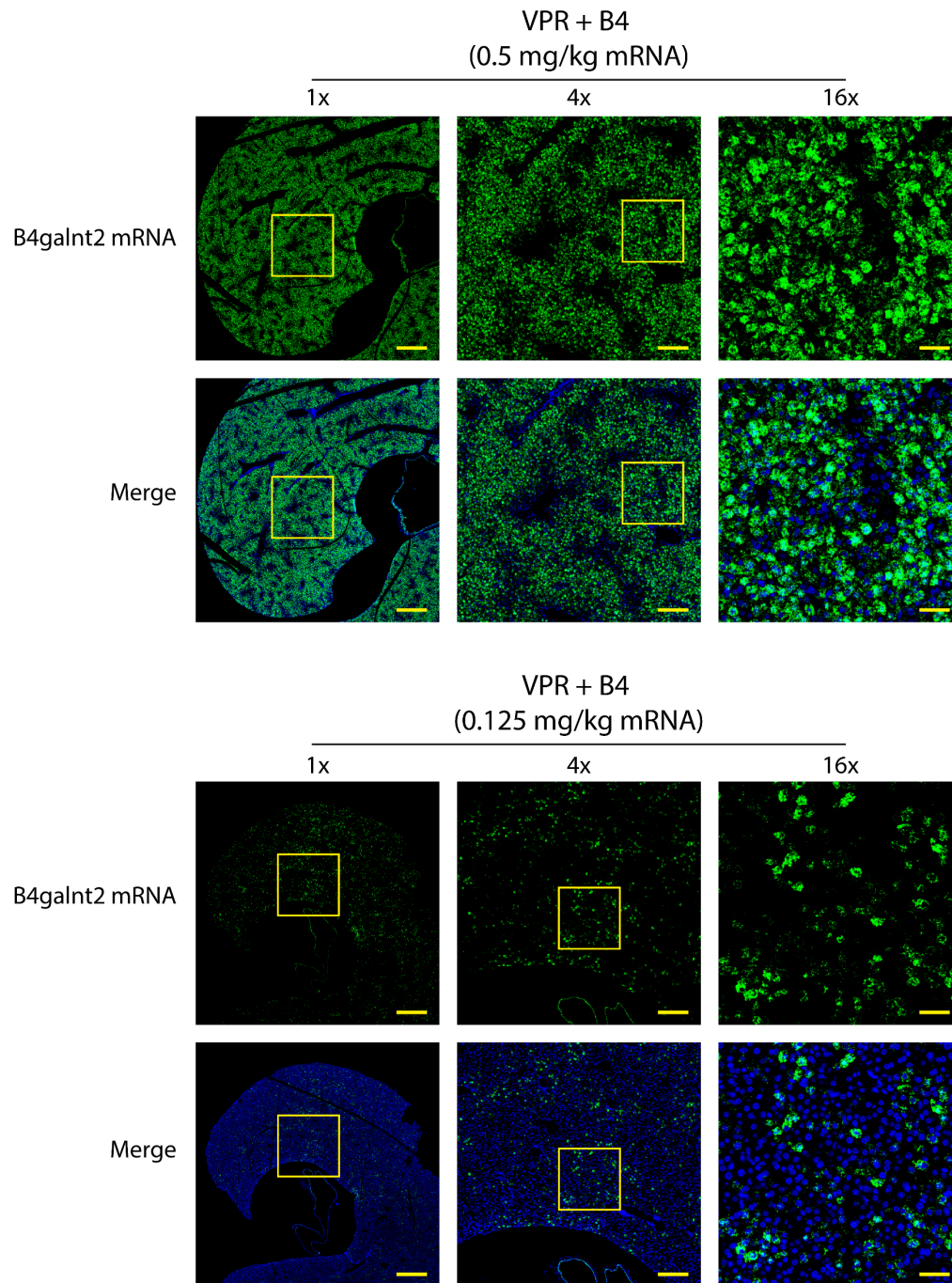
b



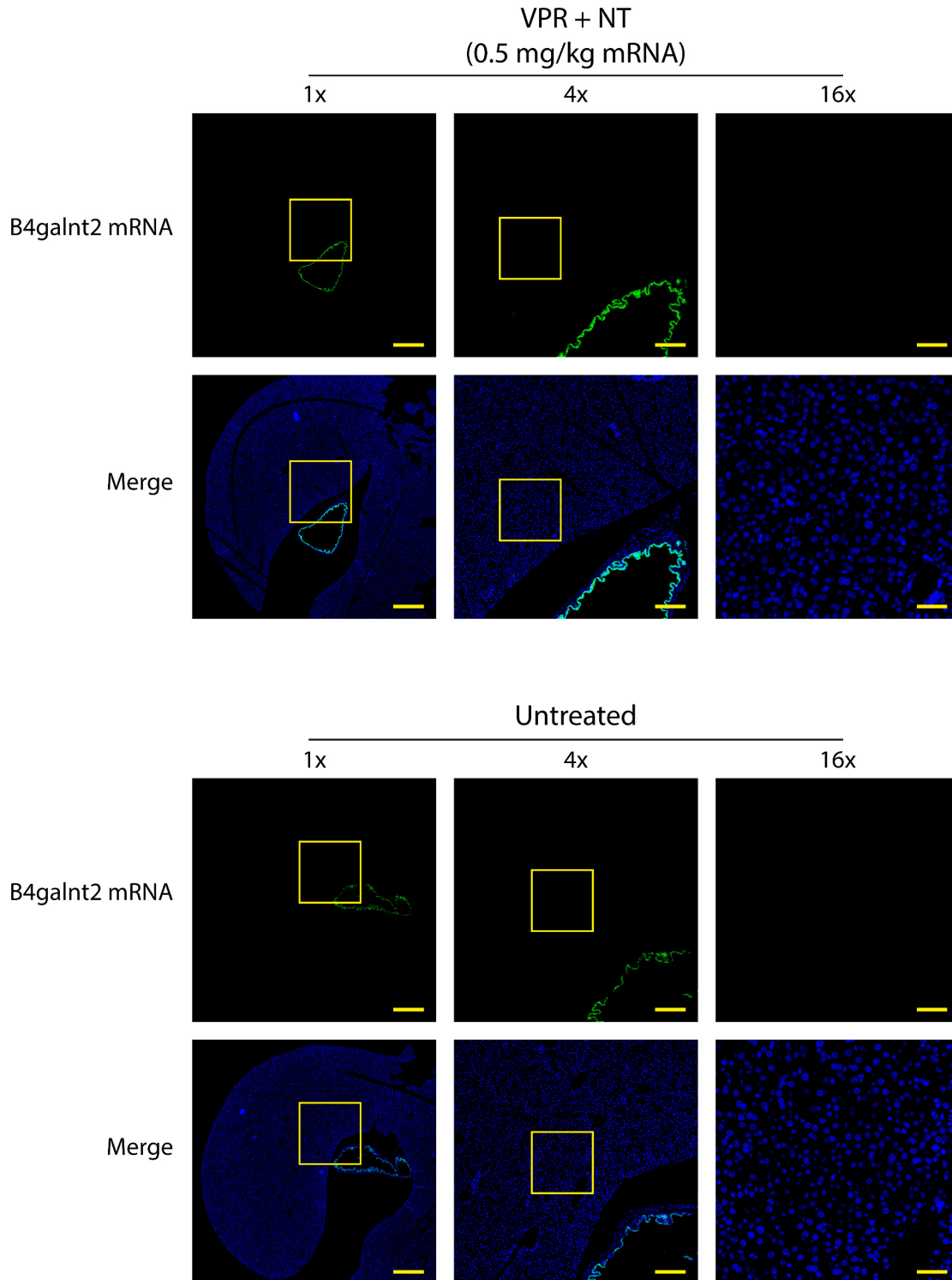
Sup. Fig. 10 | Comparison of LNP formulation approaches. a, B4galnt2 mRNA copy numbers in bulk hepatocytes (a) and percentage of activated hepatocytes (b) between combined and separate formulation approaches at a dose of 1 mg/kg VPR mRNA. Data represent mean \pm SEM (n = 3-4 mice). Statistical significance was assessed using a two-way ANOVA followed by Dunnett's multiple comparison between formulation approaches.

a**b****c****d**

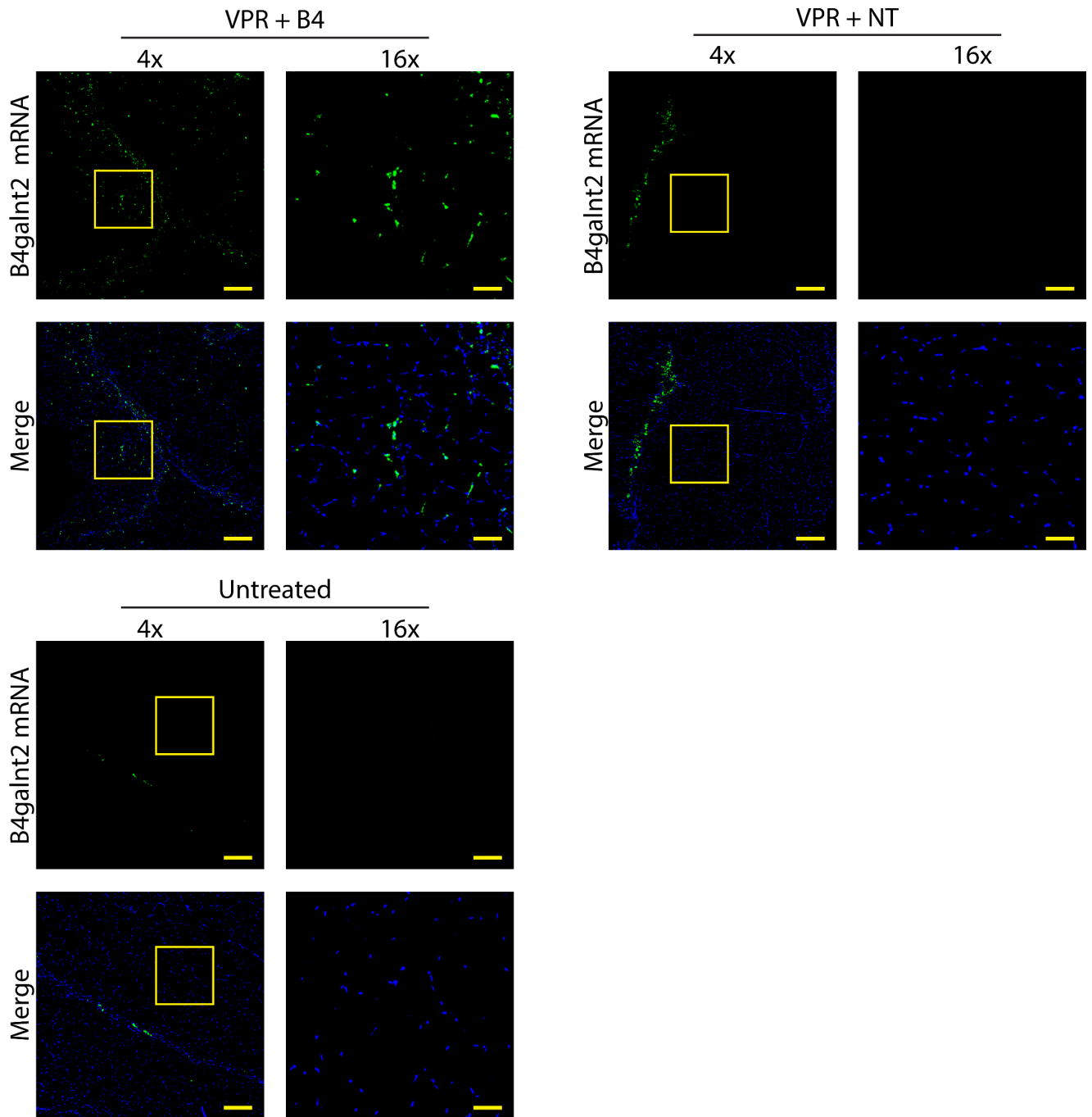
Sup. Fig. 11 | mRNA and sgRNA titration for B4galnt2 gene activation. (a, b) Titration results from fixed mRNA at 0.5 mg/kg and varying sgRNA:mRNA ratio between 1:3 and 3:1. (c, d) Titration results from fixed sgRNA at 0.5 mg/kg and varying sgRNA:mRNA ratio between 1:3 and 3:1. Data represent mean \pm SEM (n = 3-4 mice). Statistical significance was assessed using a one-way ANOVA followed by Dunnett's multiple comparison between each B4 treatment dose and a sgRNA:mRNA mass ratio of 3 (a, b) or a mass ratio of 1:3 (c, d). (*P<0.05, **P<0.01, ***P<0.001, ****P<0.0001).



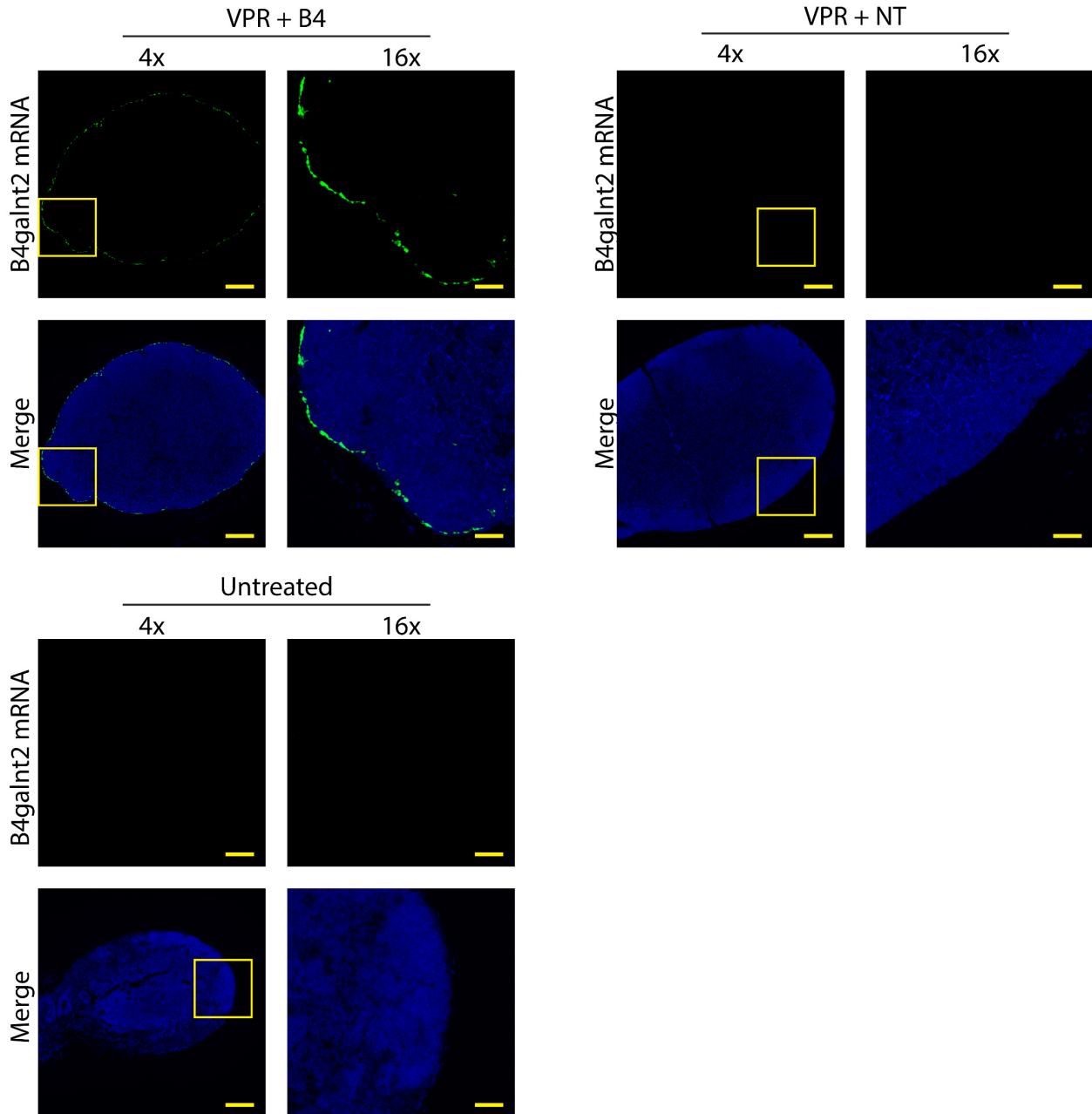
Sup. Fig. 12 | Representative slide scan images of B4galnt2 mRNA upregulation at 0.5 mg/kg and 0.125 mg/kg mRNA dose. Representative slide scan images of liver sections showing RNAscope staining for B4galnt2 mRNA (green) and DAPI (blue). The 0.125 mg/kg dose included in this figure is not contained in Figure 3a. Insets depict the relative locations of 4x and 16x views. Scale bars are 800 μ m for 1x, 200 μ m for 4x, and 50 μ m for 16x images.



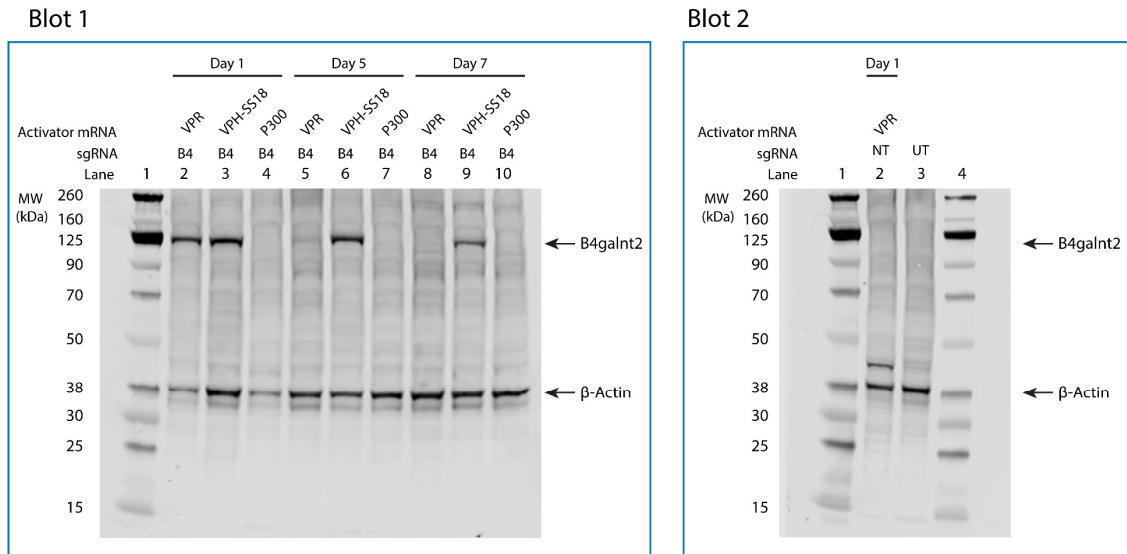
Sup. Fig. 13 | Representative slide scan images of non-targeted control and untreated livers. Representative slide scan images of liver sections showing RNAscope staining for B4galnt2 mRNA (green) and DAPI (blue). The untreated condition included in this figure is not contained in Figure 3a. Insets depict the relative locations of 4x and 16x views. Scale bars are 800 μ m for 1x, 200 μ m for 4x, and 50 μ m for 16x images. Basal B4galnt2 mRNA expression occurs in untreated mice in the gallbladder.



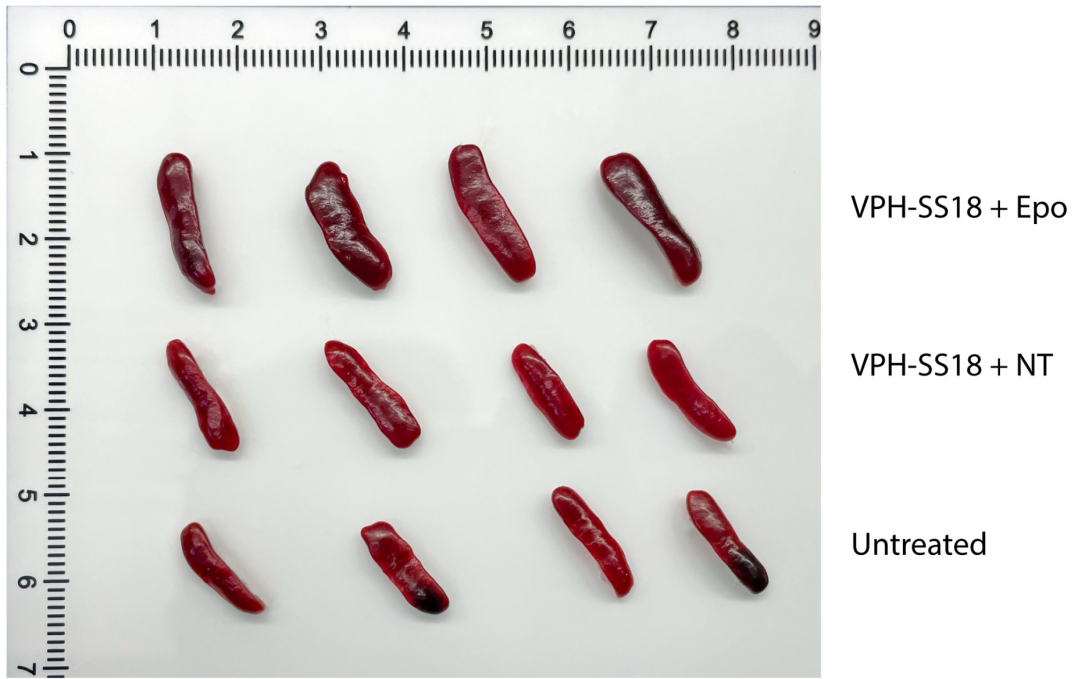
Sup. Fig. 14 | Representative slide scan images of B4galnt2 mRNA upregulation in the quadriceps muscle. Representative slide scan images of quadriceps muscle sections showing RNAscope staining for B4galnt2 mRNA (green) and DAPI (blue). The VPR mRNA + B4 sgRNA treatment group displays multiple activated cells within the muscle fibers. . Insets depict the relative locations of 16x views. Scale bars are 200 μ m for 4x and 50 μ m for 16x images



Sup. Fig. 15 | Representative slide scan images of B4galnt2 mRNA upregulation in the paraaortic lymph node. Representative slide scan images of paraaortic lymph node showing RNAscope staining for B4galnt2 mRNA (green) and DAPI (blue). The VPR mRNA + B4 sgRNA treatment group displays a strong ring of activated cells surrounding the lymph node. Insets depict the relative locations of 16x views. Scale bars are 200 μm for 4x and 50 μm for 16x images



Sup. Fig. 16 | Western blot images of B4galnt2 protein upregulation in liver samples. Liver lysates were assessed for B4galnt2 protein, the dimeric protein (~125 kDa) is visible at ~125 kDa (63.25 kDa monomer) and actin (~38 kDa). Lanes are labeled with the activator mRNA and sgRNA injected into each animal. Blot 1, lane 1 and Blot 2 lanes 1 and 4 contain molecular weight ladders. Blot 2, lane 3 represents an untreated mouse.



Sup. Fig. 17 | Spleen images of from all mice 7 days post injection. Ambient light images of spleens are organized by rows. Scale markers represent 1 cm.